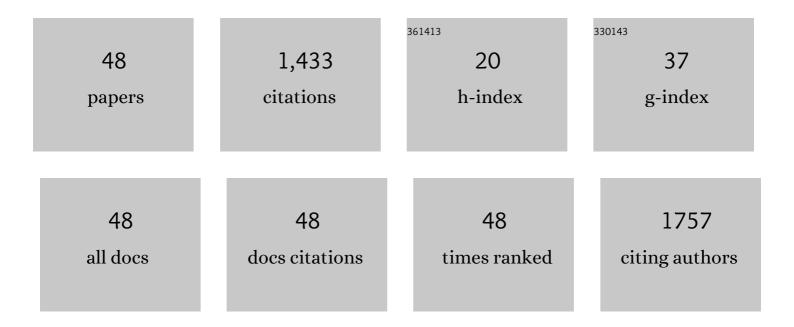
Ji-min yang

List of Publications by Year in descending order

Source: https://exaly.com/author-pdf/1969078/publications.pdf Version: 2024-02-01



ILMIN VANC

#	Article	IF	CITATIONS
1	Functionally modified metal–organic frameworks for the removal of toxic dyes from wastewater. CrystEngComm, 2022, 24, 434-449.	2.6	17
2	MIL-100(Fe)@GO composites with superior adsorptive removal of cationic and anionic dyes from aqueous solutions. Journal of Molecular Structure, 2022, 1265, 133365.	3.6	7
3	Sulfo-modified MIL-101 with immobilized carbon quantum dots as a fluorescence sensing platform for highly sensitive detection of DNP. Inorganica Chimica Acta, 2021, 519, 120276.	2.4	9
4	Superior adsorptive removal of azo dyes from aqueous solution by a Ni(II)-doped metal–organic framework. Colloids and Surfaces A: Physicochemical and Engineering Aspects, 2021, 619, 126549.	4.7	19
5	Rapid adsorptive removal of cationic and anionic dyes from aqueous solution by a Ce(III)-doped Zr-based metal–organic framework. Microporous and Mesoporous Materials, 2020, 292, 109764.	4.4	56
6	Surface-Functionalized MoS ₂ Nanosheets Sensor for Direct Electrochemical Detection of PIK3CA Gene Related to Lung Cancer. Journal of the Electrochemical Society, 2020, 167, 027501.	2.9	13
7	Modulation of the driving forces for adsorption on MIL-101 analogues by decoration with sulfonic acid functional groups: superior selective adsorption of hazardous anionic dyes. Dalton Transactions, 2020, 49, 6651-6660.	3.3	29
8	Modulation of driving forces fo UiO-66 analog adsorbents by decoration with amino functional groups: Superior adsorption of hazardous dyes. Journal of Molecular Structure, 2020, 1220, 128716.	3.6	15
9	Self-Signal Electrochemical Monitoring of Hybridization of Nucleic Acids Based on Riboflavine Sodium Phosphate Decorated WS ₂ Nanosheets. Journal of the Electrochemical Society, 2020, 167, 027502.	2.9	7
10	Effect of Synergistic Interplay between Surface Charge, Crystalline Defects, and Pore Volume of MIL-100(Fe) on Adsorption of Aqueous Organic Dyes. Industrial & Engineering Chemistry Research, 2020, 59, 2113-2122.	3.7	44
11	Superior selective adsorption of anionic organic dyes by MIL-101 analogs: Regulation of adsorption driving forces by free amino groups in pore channels. Journal of Molecular Liquids, 2020, 302, 112616.	4.9	32
12	Fabrication of a carbon quantum dots-immobilized zirconium-based metal-organic framework composite fluorescence sensor for highly sensitive detection of 4-nitrophenol. Microporous and Mesoporous Materials, 2019, 274, 149-154.	4.4	84
13	Superior adsorptive removal of anionic dyes by MIL-101 analogues: the effect of free carboxylic acid groups in the pore channels. CrystEngComm, 2019, 21, 5824-5833.	2.6	15
14	Electrochemical determination of PIK3CA gene associated with breast cancer based on molybdenum disulfide nanosheet-supported poly(indole-6-carboxylic acid). Analytical Methods, 2019, 11, 157-162.	2.7	10
15	Construction of self-signal DNA electrochemical biosensor employing WS ₂ nanosheets combined with PIn6COOH. RSC Advances, 2019, 9, 9613-9619.	3.6	13
16	Effect of free carboxylic acid groups in UiO-66 analogues on the adsorption of dyes from water: Plausible mechanisms for adsorption and gate-opening behavior. Journal of Molecular Liquids, 2019, 283, 160-166.	4.9	38
17	Highly Sensitive and Selective Detection of 2,4-Dinitrophenol by a Fluorescent Amine-Functionalized Carbon Quantum Dot@Metal-Organic Framework. Russian Journal of Physical Chemistry A, 2019, 93, 2452-2457.	0.6	7
18	Effect of surface charge status of amorphous porous coordination polymer particles on the adsorption of organic dyes from an aqueous solution. Journal of Colloid and Interface Science, 2018, 525, 54-61.	9.4	40

JI-MIN YANG

#	Article	IF	CITATIONS
19	High-performance electrochemical sensing of circulating tumor DNA in peripheral blood based on poly-xanthurenic acid functionalized MoS 2 nanosheets. Biosensors and Bioelectronics, 2018, 105, 116-120.	10.1	61
20	Adsorptive removal of organic dyes from aqueous solution by a Zr-based metal–organic framework: effects of Ce(<scp>iii</scp>) doping. Dalton Transactions, 2018, 47, 3913-3920.	3.3	161
21	Tungsten disulfide nanosheets supported poly(xanthurenic acid) as a signal transduction interface for electrochemical genosensing applications. RSC Advances, 2018, 8, 39703-39709.	3.6	9
22	Effect of the Synergetic Interplay between the Electrostatic Interactions, Size of the Dye Molecules, and Adsorption Sites of MIL-101(Cr) on the Adsorption of Organic Dyes from Aqueous Solutions. Crystal Growth and Design, 2018, 18, 7533-7540.	3.0	62
23	Effect of particle size distribution of UiO-67 nano/microcrystals on the adsorption of organic dyes from aqueous solution. CrystEngComm, 2018, 20, 5672-5676.	2.6	10
24	A facile approach to fabricate an immobilized-phosphate zirconium-based metal-organic framework composite (UiO-66-P) and its activity in the adsorption and separation of organic dyes. Journal of Colloid and Interface Science, 2017, 505, 178-185.	9.4	88
25	Controlled growth and DNA sensing property of HKUST-1@GrO nanocomposites. Materials Letters, 2017, 209, 142-145.	2.6	2
26	MOF-derived hollow NiO–ZnO composite micropolyhedra and their application in catalytic thermal decomposition of ammonium perchlorate. Russian Journal of Physical Chemistry A, 2017, 91, 1214-1220.	0.6	13
27	Facile water-stability evaluation of metal–organic frameworks and the property of selective removal of dyes from aqueous solution. Dalton Transactions, 2016, 45, 8753-8759.	3.3	76
28	Shape-controlled synthesis and photocatalytic activity of In 2 O 3 nanostructures derived from coordination polymer precursors. Chinese Chemical Letters, 2016, 27, 492-496.	9.0	26
29	Metal ion induced porous HKUST-1 nano/microcrystals with controllable morphology and size. CrystEngComm, 2016, 18, 4127-4132.	2.6	40
30	Facile fabrication of MIL-103(Eu) porous coordination polymer nanostructures and their sorption and sensing properties. Dalton Transactions, 2016, 45, 5841-5847.	3.3	26
31	Effect of additives on morphology and size and gas adsorption ofÂSUMOF-3 microcrystals. Microporous and Mesoporous Materials, 2016, 222, 27-32.	4.4	15
32	A facile approach to fabricate porous UMCM-150 nanostructures and their adsorption behavior for methylene blue from aqueous solution. CrystEngComm, 2015, 17, 4825-4831.	2.6	17
33	Morphology evolution and gas adsorption of porous metal–organic framework microcrystals. Dalton Transactions, 2015, 44, 16888-16893.	3.3	12
34	Controlled growth and gas sorption properties of IRMOF-3 nano/microcrystals. Dalton Transactions, 2014, 43, 16707-16712.	3.3	26
35	The phase equilibriums in the NH4Cl-CaCl2-H2O system at 50 and 75°C and their Pitzer model representations. Russian Journal of Physical Chemistry A, 2014, 88, 2325-2330.	0.6	4
36	Shape and size control and gas adsorption of Ni(II)-doped MOF-5 nano/microcrystals. Microporous and Mesoporous Materials, 2014, 190, 26-31.	4.4	77

JI-MIN YANG

#	Article	IF	CITATIONS
37	Cucurbit[6]uril-Based Supramolecular Assemblies: Possible Application in Radioactive Cesium Cation Capture. Journal of the American Chemical Society, 2014, 136, 16744-16747.	13.7	82
38	Co(II)-doped MOF-5 nano/microcrystals: Solvatochromic behaviour, sensing solvent molecules and gas sorption property. Journal of Solid State Chemistry, 2014, 218, 50-55.	2.9	47
39	Porous ZnO and ZnO–NiO composite nano/microspheres: synthesis, catalytic and biosensor properties. RSC Advances, 2014, 4, 51098-51104.	3.6	14
40	Controlled Synthesis of Porous Coordinationâ€Polymer Microcrystals with Definite Morphologies and Sizes under Mild Conditions. Chemistry - A European Journal, 2014, 20, 14783-14789.	3.3	53
41	Solid-liquid phase equilibria at 50 and 75°C in the NaCl + MgCl2 + H2O system and the pitzer model representations. Russian Journal of Physical Chemistry A, 2013, 87, 2195-2199.	0.6	4
42	The phase diagrams and Pitzer model representations for the system KCl + MgCl2 + H2O at 50 and 75°C. Russian Journal of Physical Chemistry A, 2012, 86, 1930-1935.	0.6	6
43	Solubilities of salts in the ternary systems NaCl + CaCl2 + H2O and KCl + CaCl2 + H2O at 75°C. Russian Journal of Physical Chemistry A, 2011, 85, 1149-1154.	0.6	11
44	Solubility in the ternary system LiCl + MgCl2 + H2O at 60 and 75°C. Russian Journal of Physical Chemistry A, 2010, 84, 1169-1173.	0.6	11
45	Measurement of Solubilities in the Ternary System NaCl + CaCl2+ H2O and KCl + CaCl2+ H2O at 50℃. Journal of the Korean Chemical Society, 2010, 54, 269-274.	0.2	11
46	Osmotic Coefficients of the Li2B4O7+LiCl + H2O System at T=273.15 K. Journal of Solution Chemistry, 2009, 38, 429-439.	1.2	4
47	Isopiestic Determination of the Osmotic Coefficients andÂPitzer Model Representation forÂtheÂLi2B4O7+LiCl + H2O System at T=298.15ÂK. Journal of Solution Chemistry, 2008, 37, 377-389.	1.2	10
48	Electrochemical self-signal switch for determination of KRAS gene employingÂriboflavin 5'-adenosine diphosphate functionalized MoS2 nanosheets. Journal of Solid State Electrochemistry, 0, , 1.	2.5	0